Lab on a Chip

CRITICAL REVIEW

View Article Online
View Journal | View Issue

Cite this: *Lab Chip*, 2024, **24**, 1226

Microfluidic synthesis of radiotracers: recent developments and commercialization prospects

Mark Mc Veigh [a] and Leon M. Bellan *[bc]

Positron emission tomography (PET) is a powerful diagnostic tool that holds incredible potential for clinicians to track a wide variety of biological processes using specialized radiotracers. Currently, however, a single radiotracer accounts for over 95% of procedures, largely due to the cost of radiotracer synthesis. Microfluidic platforms provide a solution to this problem by enabling a dose-on-demand pipeline in which a single benchtop platform would synthesize a wide array of radiotracers. In this review, we will explore the field of microfluidic production of radiotracers from early research to current development. Furthermore, the benefits and drawbacks of different microfluidic reactor designs will be analyzed. Lastly, we will discuss the various engineering considerations that must be addressed to create a fully developed, commercially effective platform that can usher the field from research and development to commercialization.

Received 14th September 2023,
Accepted 22nd November 2023

DOI: 10.1039/d3lc00779k

rsc.li/loc

Introduction

In the early 1900s, George de Hevesy used lead isotopes to track the metabolic use of lead by plants, earning him the 1943 Nobel Prize in Chemistry.[1] The medical field noted the incredible potential of using radioactivity to track metabolic processes, and so this technology concept was further refined to a point that in the 1970s, the first positron emission tomography (PET) scanners were developed.[1] PET works by injecting a patient with a radiotracer (a biomolecule labeled with a radionuclide[2]), and as the radiotracer travels through the body, the radionuclide decays and releases a positron *via* β^+ decay (Fig. 1).[3] The positron travels only a short distance until it is annihilated by an electron.[4] This annihilation event releases a pair of anti-parallel photons that are then captured by detectors in the PET scanner. Both photons must be detected within a tight spatial and temporal window to confirm they are produced from the same event.[5] Using this

[a] *Interdisciplinary Materials Science Program, Vanderbilt University, Nashville, TN, 37235, USA*
[b] *Department of Mechanical Engineering, Vanderbilt University, Nashville, TN, 37235, USA. E-mail: leon.bellan@vanderbilt.edu*
[c] *Department of Biomedical Engineering, Vanderbilt University, Nashville, TN 37235, USA*

Mark Mc Veigh

Mark Mc Veigh is a second year Ph.D. student at Vanderbilt University in the Interdisciplinary Materials Science program. He received his B.S. and M.S. in Chemical Engineering at Northeastern University in 2022. At Northeastern, he gained a wide breadth of research experience through several co-ops including formulating carbon nanotube inks, optimizing continuous heterogeneous crystallization conditions, and developing a high throughput production process for an exosome characterization platform. In pursuing his Ph.D., Mark is working in Dr. Bellan's lab on developing a novel platform for automated microfluidic synthesis of radiotracers.

Leon M. Bellan

Dr. Leon M. Bellan is an Associate Professor in the Mechanical Engineering and Biomedical Engineering departments at Vanderbilt University. He received his B.S. in Physics at Caltech in 2003 and his Ph.D. in Applied and Engineering Physics at Cornell in 2008. Before joining the faculty at Vanderbilt in 2013, he was a postdoctoral researcher at MIT. His research focuses on engineering the microvasculature, novel applications of thermoresponsive polymers, and microfluidic radiotracer production. Dr. Bellan is an author or co-author on over 60 scientific publications and an inventor on 5 US patents.

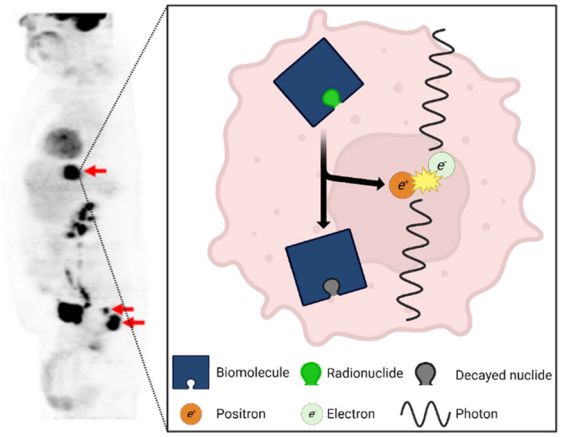

Fig. 1 The results of a PET scan using the radiotracer [^{18}F]FDG of a patient with colorectal cancer. Used with permission of Springer Nature from ref. 8; permission conveyed through Copyright Clearance Center, Inc. The most common PET radiotracers undergo β^+ decay in which a proton decays into a neutron, neutrino (not pictured), and positron. The positron travels a short distance before it is annihilated by an electron which releases a pair of anti-parallel 511 keV photons.

data, the location of the event can be identified and, after many events have been detected, a full heat map can be reconstructed, highlighting areas where the biomolecule and attached radionuclide are highly concentrated (Fig. 1). PET has become a critical diagnostic tool for physicians, especially for the diagnosis of cancer.[6] The technology continues to become more popular and accessible across the world, with 2.4 million procedures completed worldwide in 2010 increasing to over 4.9 million in 2020.[7]

The term "radiotracer" refers to the general configuration of a biomolecule labeled with a radionuclide. "Radiopharmaceuticals" are defined as the subset of radiotracers that are federally approved for clinical use (diagnostic or therapeutic).[2] The terms have often been used interchangeably but for the purposes of this review, radiotracer (tracer/probe) will be used as it encompasses all radioactively labeled compounds.

Radiotracers act as a vehicle to deliver a radionuclide to an area of interest based on the specific biological process the targeting biomolecule is involved in. Researchers can theoretically leverage any biological mechanism to achieve highly specific delivery by labeling a molecule involved in the process. For example, radiotracers can be synthesized that track physical transport throughout the body ([^{15}O]H_2O), experience increased metabolization by problematic cells ([^{18}F]FDG), or bind to an overexpressed antigen ([^{68}Ga]Ga-PSMA-11).[6] Capitalizing on this expansive design space, extraordinary amounts of research have gone into developing novel radiotracers, with over 4000 unique probes developed through 2017[9] and novel probes continuously in development. By design, many of these radiotracers have very high specificity to particular biological processes or interactions (a clear benefit of this technology). While extremely useful in specific clinical circumstances, these less-generalizable radiotracers would likely be used infrequently and thus have been referred to as "boutique tracers". With such a wide-reaching catalogue of radiotracers, PET holds unmatched potential to provide patients with personalized diagnoses and treatments (so-called "precision medicine").

While there are a myriad of probes developed in and available to research labs, physicians in the clinic are often limited to only [^{18}F]fluorodeoxyglucose ([^{18}F]FDG), a glucose molecule labelled with ^{18}F.[9] Radiolabelled glucose is an attractive choice as a broadly effective radiotracer because of the Warburg effect, which describes how cancer cells greatly increase glucose uptake compared to healthy cells.[10] For this reason, roughly 95% of PET scans use [^{18}F]FDG.[9] However, glucose is used generally throughout the body during normal, healthy metabolism, and its use may be elevated in non-cancerous conditions such as inflammation or infection. This means that [^{18}F]FDG is not highly selective and can lead to false-positives.[6]

To overcome this, clinicians can turn to a number of clinically relevant probes. For example, (*S*)-4-(3-[^{18}F]fluoropropyl)-L-glutamic acid ([^{18}F]FSPG), a glutamine analogue, has recently gained popularity due to its highly specific uptake in certain cancers which results in a much greater contrast than [^{18}F]FDG.[6] Outside the realm of cancer diagnostics, high natural uptake of [^{18}F]FDG in healthy brain tissue reduces its ability to differentiate metabolism in the brain of patients with Alzheimer's disease against patients with other dementia disorders.[11] Due to such issues, researchers have developed more specific and thus more effective tracers like [^{18}F]flutemetamol, which targets amyloid plaques in the brain, to improve the diagnosis and treatment of patients with cognitive impairment.[12] Further discussion of clinically relevant non-[^{18}F]FDG radiotracers can be found in multiple papers.[6,13,14]

Even with these more targeted options, [^{18}F]FDG continues to dominate the market because of its effectiveness across many types of cancer and the economic difficulty of producing other radiotracers. As will be discussed further, the cost of building and maintaining current radiotracer production infrastructure is so high that most clinically-oriented facilities rely on economy of scale to maintain profitability.[15] The current production model and associated equipment are designed for high-volume production of a single radiotracer, rendering it infeasible to produce an array of highly specific radiotracers in low volumes.

In addition to diagnostic imaging, radiotracers are being developed as theranostic pairs. The premise of radiotheranostics is to capitalize on the different decay modes and rates of radionuclides to create a diagnostic and therapeutic pair. For diagnostics, it is preferable to use lower energy, positron emitting radionuclides with relatively shorter half-lives. For the therapeutic counterpart, higher energy, α- or β^- emitting radionuclides with longer half-lives are chosen to produce extended attacks on the target tissue.[16] This approach has been used for decades, most prominently employing the ^{124}I and ^{131}I pair to diagnose and treat thyroid cancers, respectively.[17] Again, the current clinical production

model cannot sustain affordably-priced production beyond [^{18}F]FDG, limiting the ability to provide physicians with an effective suite of radiotheranostic options.

To shift PET to a precision medicine platform, patients must have inexpensive access to the wide range of radiotracers described in scientific literature and those yet to be discovered. A localized dose-on-demand strategy has been the leading plan to provide this. By transitioning radiotracer synthesis from multi-dose to single dose batches, local scanning facilities could produce their doses on-site, significantly lowering the expenses for patients. For nearly 20 years, microfluidics has been proposed as the best route to achieve this goal. However, difficulties in achieving complete microfluidic integration of all radiosynthesis steps, interfacing macro- and microfluidic components, and building a fully automated unit have slowed the widespread commercialization of microfluidics-based platforms. In this review, we will first discuss the current state of the art. Then, we will analyze the efforts to develop microfluidic platforms by reviewing early projects, exploring the benefits and limitations of current work, and finally discussing additional considerations necessary for commercialization.

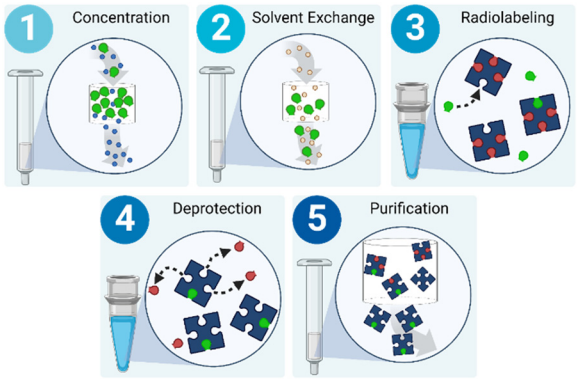

Fig. 2 Radiosyntheses involving ^{18}F tend to follow the same generic procedure. Effectively concentrating the radionuclide produced by a cyclotron or generator is critical for economic use of the radioactive material. After the radionuclide is eluted, an evaporative step is performed to remove all residual water. Once the radionuclide is fully dried, the radiolabeling solvents and reagents are introduced. Some compounds have multiple sites available for radionuclide binding, so protection (off-chip) and deprotection (post-radiolabeling) of these sites with less reactive moieties is common.

Commercial production of [^{18}F]FDG and other tracers

Currently, centralized production facilities are responsible for generating radionuclides (*i.e.* ^{18}F, ^{11}C, ^{68}Ga, *etc.*),[18] chemically bonding them to or otherwise incorporating them with biomolecules to create radiotracers, and performing all necessary quality control (QC) tests to create a safe and well-characterized patient-ready dose. ^{18}F, the most common radionuclide for radiotracers, is generated in a cyclotron *via* the ^{18}O(p,n)^{18}F reaction in which [^{18}O]H_2O is bombarded with protons resulting in a water-based solution containing ^{18}F.[19] The radioactive product of the cyclotron (or generator for other radionuclides[20]) can be plumbed directly to nearby hot cells containing commercial radiotracer synthesis modules. Hot cells are large, expensive, lead-lined chambers that protect the operator as they handle radioactive material using externally controlled manipulators. Before any production can be executed within the hot cell, the synthesis module must be extensively prepared by a highly trained operator.

Although there are variations in solvents, reaction temperatures, and post-labeling reactions, radiosyntheses follow a generic process: solution preparation, radiolabeling, secondary reactions, and purification. In particular, the majority of radiosyntheses involving ^{18}F can be described with a slightly more defined process flow (Fig. 2). First, the radionuclide must be concentrated into whatever solvent is necessitated by the radiochemistry. This is often completed using a combination of solid phase extraction (SPE) and evaporation.[21] SPE requires a packed bed of exchange medium, and evaporation requires a heated chamber equipped with gas inlets and vacuum outlets to assist in mass transfer of the solvent to be removed. Next, the necessary precursors and solvents are introduced into the system and reacted to radiolabel the biomolecule of interest. Radiolabeling often requires a heated chamber to drive the reaction. After labeling, some reactions require a deprotection step that also necessitates a temperature-controlled chamber. Finally, the radiotracer must be purified to produce a usable dose; this is most often accomplished *via* either HPLC or SPE using another packed bed.[22,23] The exact design of each synthesis module varies, but, importantly, they all contain the necessary unit operations to execute a complete synthesis.

There are several metrics employed to report the level of success of a synthesis run. The most reported, and arguably most important, is radiochemical yield (RCY). This metric is defined as the ratio of the activity in the final material to the activity of starting material.[24] Unless otherwise specified, RCY is decay corrected meaning any losses of activity due to decay do not contribute to the metric. Additionally, radiochemical purity is the percentage of radioactivity of a product that comes from the desired radiotracer as opposed to free radionuclide or radioactive by-products.[25]

Once the radiotracer is synthesized, it must pass QC to ensure that it meets certain criteria mandated by locally applicable regulatory bodies. Per the US Pharmacopeia, the criteria are appearance, radionuclide and radiochemical identity, bacterial endotoxins, pH, radiochemical, radionuclide, and chemical purity, residual solvents, and sterility.[25] If these criteria are satisfied, the doses are packaged and distributed to nearby hospitals and scanner centers. The scanning facilities have no part in the production process and receive the doses ready-to-use. Given the rapid decay of the radionuclides involved, it is critical

that every step of the process is completed as fast as possible to maintain enough radioactivity for proper dosing.

The current pipeline for radiotracer production was developed when there were fewer alternatives to [^{18}F]FDG, so it was only natural to create systems that would profit the most from producing it at the highest rate possible. To ensure that PET was reasonably affordable, it was logical to design equipment to synthesize large batches of the dominant radiotracer.[26] The pipeline was also effective in supporting increasing [^{18}F]FDG demand as PET usage continued to grow. Production facilities could easily increase their [^{18}F]FDG throughput by increasing the amount of bombardment time in the cyclotron to produce more ^{18}F. Now, however, with so many novel radiotracers developed, this economic strategy is no longer optimal.

There are several standard production platforms such as the TracerLab (GE Healthcare), FASTLab (GE Healthcare), iPhase MultiSyn (iPHASE Technologies), Modular-Lab Standard (Eckert & Ziegler), and the AllinOne (Trasis). These platforms can generally be categorized as either a fully plumbed or cassette-based system. GE's TracerLab is a very popular example of a fully plumbed synthesis module, designed to repeatedly run the same synthesis. By having a large amount of plumbing between various removable unit operation components (ion exchange columns, reaction vessels, *etc.*), the TracerLab is well designed for repeatedly executing large-scale production runs of [^{18}F]FDG. The module also has the ability to decontaminate itself in an automated fashion, minimizing the dead time between runs, and enabling high volume production. However, the process of reconfiguring fully plumbed modules to switch to a new synthesis approach requires a well-trained operator, is quite complicated, and is highly time-consuming, rendering boutique tracer production impractical and not economically viable.

GE's FASTlab is an example of an effective cassette-based module that allows for an immense amount of customizability between each run without any replumbing. A cassette is initially prepared by an operator so that it contains all the necessary solvents and unit operations (SPE cartridges, reaction chambers, *etc.*) for the given synthesis. The single use nature of the cassette limits its financial benefit for [^{18}F]FDG because of the additional cost of each cassette. However, cassettes are much easier to replace than replumbing an entire system, so the design makes it an ideal module for synthesizing less common tracers. Cassette based systems are well suited for boutique tracer synthesis but are difficult to employ for dose-on-demand production at reasonable cost due to large reagent volumes, long dead times between runs due to substantial preparation, and high cost of shielding.

Microfluidic radiotracer production

Personalized care through dose-on-demand radiotracer production is unachievable with current manufacturing processes. To change this, microfluidic approaches have been touted as the ideal solution.[15,22,26] Microfluidic approaches require far smaller working volumes, resulting in several significant improvements. Reduced volumes lead to more controllable fluid manipulation and higher surface to volume ratios, improving heat transfer. Traditional modules use very small amounts of radioactive material and use large amounts of solvent to easily manipulate the fluid.[27] Microfluidics, on the other hand, allows for decreased volumes of solvent which, in comparison to traditional modules, increases the concentrations of active species thus increasing the reaction rate and RCY. Increased yield and transition to single-dose batches means a synthesis run can start with less activity. Minimizing the amount of activity for any given production run is crucial not only due to cost but also for the general safety of operators and facilities.

Microfluidic platforms are attractive given their potential to improve multiple technical aspects of radiotracer production. Furthermore, the most exciting prospect of the envisioned microfluidic platforms in the near future is the potential to completely transform the radiotracer production pipeline. The current system, as described earlier, relies on centralized production facilities to create and distribute every radiotracer dose. This dissuades production sites from creating any radiotracers that they can't distribute to several end users. With the successful commercialization of a compact and robust microfluidic synthesis platform, scanning facilities could create single dose (or a few doses for more common tracers) batches on an as-needed basis. This would eliminate the production site's role in synthesis and require them to only distribute raw radionuclides or ready-to-use radiolabeling sources.[28]

Developing microfluidic solutions for each of the generic steps to a radiotracer synthesis listed above can be difficult, and the integration of all of them into one cohesive unit is exceedingly complex. In early development, the radiolabeling step was understandably the central focus of most research projects, with the other steps (concentration, purification, *etc.*) often considered only tangentially for later research or performed by external equipment connected to the microfluidic platform. However, consideration and integration of all components has become more common as the field rapidly progresses towards commercialization. In this review, research projects have been divided by their reactor methodology into 1) continuous flow 2) batch and 3) droplet[22,29] approaches.

Continuous flow

Early research and development. Continuous flow systems are platforms that utilize a design in which the reagents react under flow conditions. These reactors are often fabricated in the form of serpentine microfluidic channels or a length of small-bore tubing. The biggest advantage these approaches boast is an extremely high surface to volume ratio that improves heat transfer which in turn makes radiolabeling

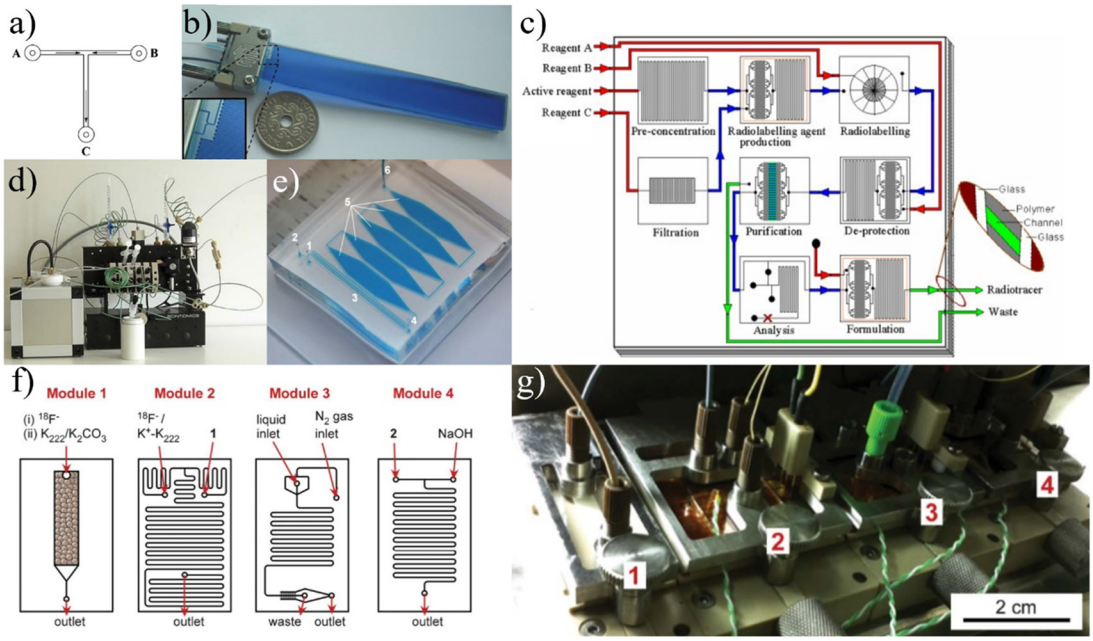

Fig. 3 Early continuous flow devices. The radiochemistry completed using the devices in a)[30] and b)[34] was instrumental in proving that radiotracer synthesis could be executed in microfluidic reactors. Building off the initial devices focused on the radiolabeling step, subsequent development focused on integrating all steps of the process. Some projects used multichip systems as in c),[35] f and g)[44] while others used fully plumbed systems d).[36] Additionally, researchers continued to modify designs to improve RCY. e)[37] One specific approach to this was to increase the reaction channel width to increase residence time. Used with permission of a, f and g) Royal Society of Chemistry from ref. 30 and 44, b and c) John Wiley & Sons from ref. 34 and 35, d and e) Springer Nature from ref. 36 and 37; permission conveyed through Copyright Clearance Center, Inc.

more efficient.[29] In 2004, Lu *et al.* reported the high first microfluidic device that was developed specifically for radiotracer synthesis.[30] The device implemented a simple T-shaped continuous flow reactor (Fig. 3a) and provided a proof of concept that radionuclides could be attached to generic organic functional groups under microfluidic flow conditions. Two years later, Gillies *et al.* reported on a multi-layered device centered around a 1 mm diameter, 100 μm tall reaction disc that acted as a continuous flow vortex mixer to produce [^{18}F]FDG with a RCY of roughly 50%.[31,32] Miller *et al.* reported on a setup using a 45 cm (1 mm diameter) reactor tube packed with palladium catalyst to execute ^{11}C-radiolabeling of various aryl halides.[33] They later changed the reactor to a microfluidic channel measuring 5 m long, 200 μm wide, and 100 μm tall (Fig. 3b) to accomplish similar palladium-catalyzed ^{11}C-radiolabelings.[34]

With it well established that the reactions necessary for radiotracer production were feasible in continuous flow reactors, groups focused on developing the technology for commercially applicable reactions. Steel *et al.* jumped directly to developing a platform that included a microfluidic module for every step of a radiosynthesis (Fig. 3c).[35] The group was able to run a fully automated synthesis of [^{18}F]FDG with a RCY of 40%. In 2008, Wester *et al.* achieved an impressive RCY of [^{18}F]FDG at 88% using an automated platform with a capillary tubing reactor (Fig. 3d).[36] In 2010, Wheeler *et al.* developed a device focused on labeling biomolecules with radiometals.[37] The reactor was constructed as a series of five "reservoirs", each measuring 5 mm in width, 3 cm in length, and 100 μm in depth (Fig. 3e). In these reservoirs, the increased volume leads to increased residence time, allowing the reaction mixture to incubate and achieve radiolabeling yields (defined by the authors as the ratio of activity from labeled ^{64}Cu to the activity of all ^{64}Cu, both labeled and unlabeled) of over 90% for the labeling of [^{64}Cu]DOTA-*cyclo*(RGDfK). This work was further optimized and automated to produce higher radiolabeling yields than conventional methods for a series of ^{64}Cu and ^{68}Ga-labeled tracers.[27]

In the mid-2010's, reports published on continuous flow microfluidics tended to focus on using relatively simplistic path designs and only addressed a portion of the synthesis process (*i.e.* concentration and labeling).[38–43] Arima *et al.* did, however, report on a multi-component platform with a series of microchannel reactors to achieve each step of a [^{18}F]FDG synthesis (Fig. 3f and g).[44] The group was able to develop a fully automated platform that incorporated pre-concentration and purification methods as well as silicon photomultiplier tubes to monitor radioactivity.[45,46]

Highly integrated/automated solutions. The Advion Nanotek was the first commercially available microfluidic platform for radiotracer production. The continuous flow platform was first sold by NanoTek before the company was purchased by Advion. The system consists of several different units, including a concentrator module, reactor module, and pump module.[47] At the core of the reactor module there are

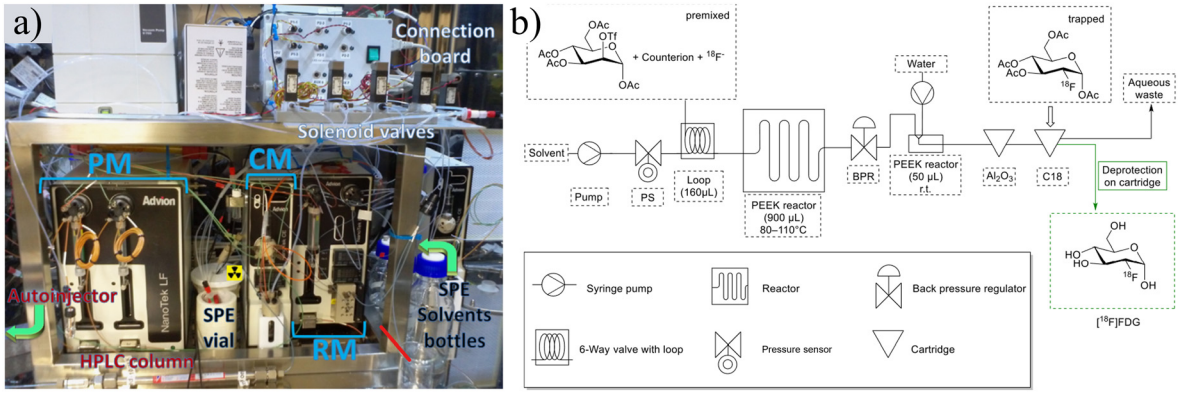

Fig. 4 a) The Advion Nanotek provides an automated method to produce radiotracers but requires significant and complicated setup. Reprinted from ref. 48 with permission from Elsevier. b) Schematic of FOMSy system with incorporated reactors and external SPE cartridges. Used with permission of Springer Nature from ref. 81; permission conveyed through Copyright Clearance Center, Inc.

four temperature-controlled locations for the user to connect continuous flow reactors of the desired length.[47] Connecting the modules are a series of eight-way distribution valves allowing the user complete control over plumbing setups. This design scheme means that the plumbing must be reconfigured for each new synthesis, which can be complicated (Fig. 4a) and time consuming.[48] The release of the Nanotek was a massive step forward for the field, with numerous research groups using the platform to synthesize a broad range of radiotracers.[47–80]

Recent/active development. Menzel *et al.* have recently released a series of papers detailing an inexpensive, 3D-printed continuous flow system named FOMSy.[81] The group first produced a proof-of-concept 3D-printed continuous flow reactor[82] and improved it by optimizing a premixing channel and transitioning the material to polyether ether ketone (PEEK) to greatly increase chemical compatibility.[83] These developments, along with the introduction of a pressure sensor and back pressure regulator, have been packaged into an automated platform designed for radiotracer synthesis (Fig. 4b).[81] The designs for all the 3D printed components are available for download. The system is very inexpensive to construct, estimated to only cost around €500 ($540). The platform was used to synthesize $[^{18}F]$FDG with a RCY over 47% and radiochemical purity over 99%.[81] The researchers, however, stated that this product is not designed for commercial production of radiotracers but rather as a low-cost and simple-to-set-up platform to conduct early-stage radiochemical research.

The field of microfluidic radiotracer production has slowly shifted interest away from continuous flow designs over the last decade (Fig. 5). The general design idea has been limited by fluidic issues such as large dead volumes, clogging and high fluidic resistance. Additionally, most radiochemical syntheses have been developed as batch processes and thus do not translate to continuous flow chemistry as easily as other approaches.[15] Continuous flow devices have fundamental drawbacks, but these are not insurmountable (as proven by some of the more advanced automated platforms). However, as will be explored further in subsequent sections, there are other reactor designs that have emerged as more favorable options. Batch devices are more analogous to traditional production methods, making them a promising option for dose-on-demand production. Droplet devices use extremely low volume for reactions, making them ideal for rapid optimization of reaction conditions. The Nanotek and other work completed on continuous flow devices prove they have potential for commercialization but, as of late, the field has more readily capitalized on the benefits of batch and droplet devices.

Batch

Early research and development. Although continuous flow was the first type of microfluidic radiotracer synthesis device developed, batch-based designs quickly followed. These designs are rather intuitive because the microfluidic

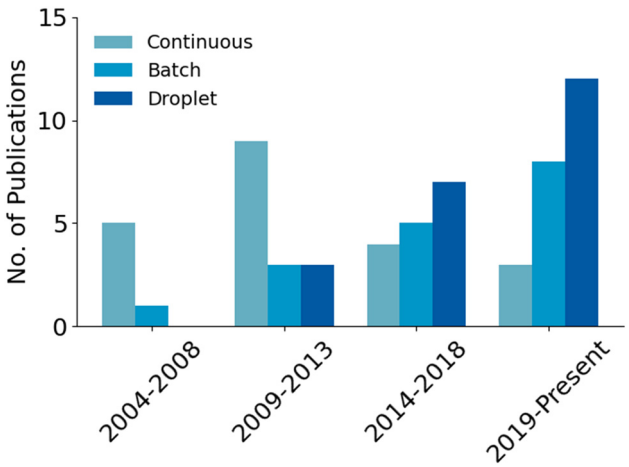

Fig. 5 Publications on the development of the various types of microfluidic devices that are cited in this review. Publications that used Advion's Nanotek to exemplify the capabilities of the machine were not included so as to focus on the developmental trends of device architectures.

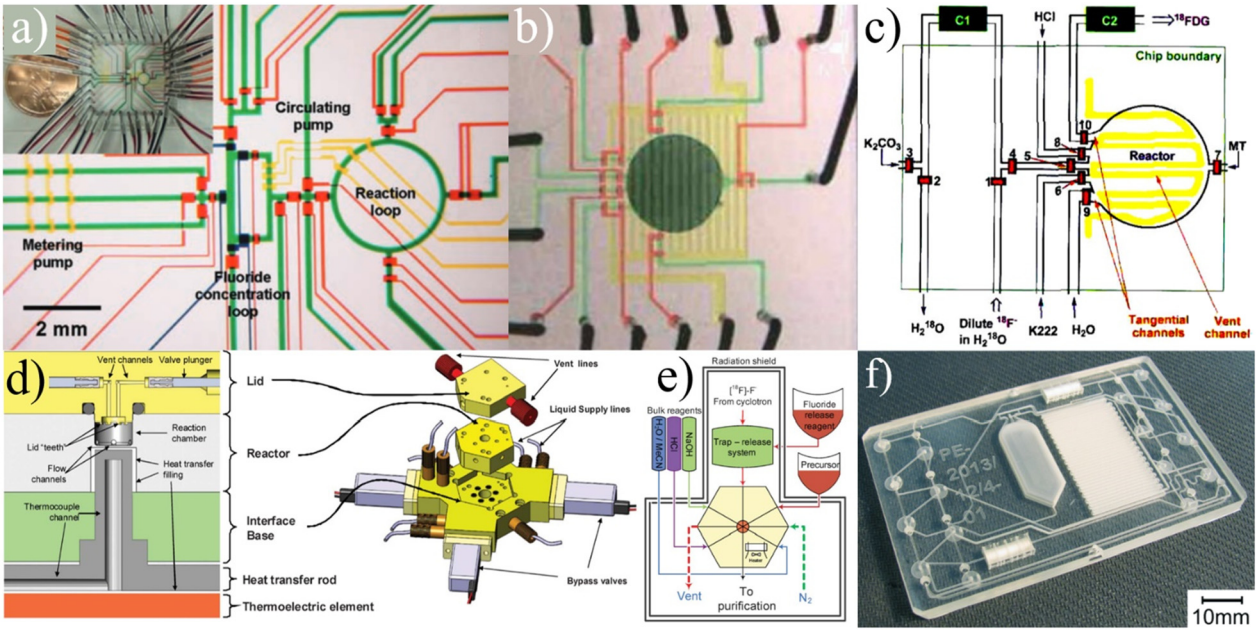

Fig. 6 a) The first iteration of batch devices were complex and unable to process substantial amounts of activity.[84] Reprinted with permission from AAAS. b and c) These concepts were subsequently developed to the point of producing full dose quantities of radiotracers.[86] This research was originally published in JNM. d and e) Further development of batch devices included additional considerations for shielding to enable the possibility of benchtop units.[88] f) The "split-box" shielding methodology was used as a fundamental design consideration while a more compact chip containing all necessary unit operations was fabricated.[89] Used with permission of Royal Society of Chemistry from ref. 88 and 89; permission conveyed through Copyright Clearance Center, Inc.

components can be directly mapped to analogous macrofluidic components on standard synthesis modules. Lee *et al.* reported the first batch-based device, developing a highly integrated design with on-chip ion exchange columns, valves, and a circular reaction loop (Fig. 6a).[84] This design was a milestone in its integration of many synthesis steps on one chip, but it could only produce 58 μCi [^{18}F]FDG as opposed to a standard human dose on the order of 10–20 mCi (based on a per mass dosage of roughly 0.2 mCi kg^{-1}).[85] This limitation was mainly an issue of processing speed, as it would have taken nearly 5 days to capture sufficient ^{18}F from 2 mL of cyclotron effluent using this approach.[86] Elizarov, the third author on the original paper, and his colleagues continued this work by developing a coin-shaped reactor that could handle the volumes necessary to concentrate ^{18}F and yield sufficient activity for multiple radiotracer doses (Fig. 6b and c).[86,87] In 2012, Lebedev *et al.* broke new ground by reporting on the first radiotracer synthesized by a microfluidic device to be injected into a human.[88] The platform was robust, containing modules for fluoride concentration, evaporation and labeling, and purification (although they were not all on a single microfluidic chip). This was the first time a platform adopted a "split-box" design, exclusively shielding the parts dealing with radioactivity (Fig. 6d and e). Selectively isolating activity-handling components increases the safety of the user and reduces costs by minimizing expensive shielding. In 2014, Rensch *et al.* demonstrated an integrated and automated platform designed around a batch reactor, isolated using on-chip valves (Fig. 6f).[89] The platform was designed specifically for a "split-box" shielding method. The microfluidic valves increased the complexity of chip fabrication and the concentration and purification columns required manual loading. The overall platform was automated with LabVIEW but struggled with occasional leaks through the conical fluidic interface to the chip.

Recent/active development. Recently, our group has been developing a series of batch microfluidic devices named RAPID (**R**adiopharmaceuticals **A**s **P**recision **I**maging **D**iagnostics). Under this platform, we have produced two similar batch devices that execute every step of the synthesis process on-chip. The first device we reported on was RAPID-F (Fig. 7a), which focused on ^{18}F chemistry and was used to synthesize clinical-grade [^{18}F]fallypride.[90] By implementing on-chip columns for both concentration and purification, the need for any macrofluidic exchange components was eliminated. To follow up, we synthesized [^{68}Ga]Ga-PSMA-11 with a similarly structured device, termed RAPID-M, that was focused on radiometal labelling (Fig. 7b).[91]

Iwata *et al.* take a rather different approach by adjusting conventional methods and equipment to integrate with a microscale batch reactor.[92] The group started by optimizing the separation of ^{18}F from [^{18}O]H_2O, focusing on using the minimum amount of solvent to achieve the ideal concentration of Kryptofix 222,[93] an organic compound that increases the reactivity of ^{18}F by binding with potassium to avoid [^{18}F]KF formation.[94] To match the scales of other microfluidic approaches,[86,87,95,96] they reduced the working

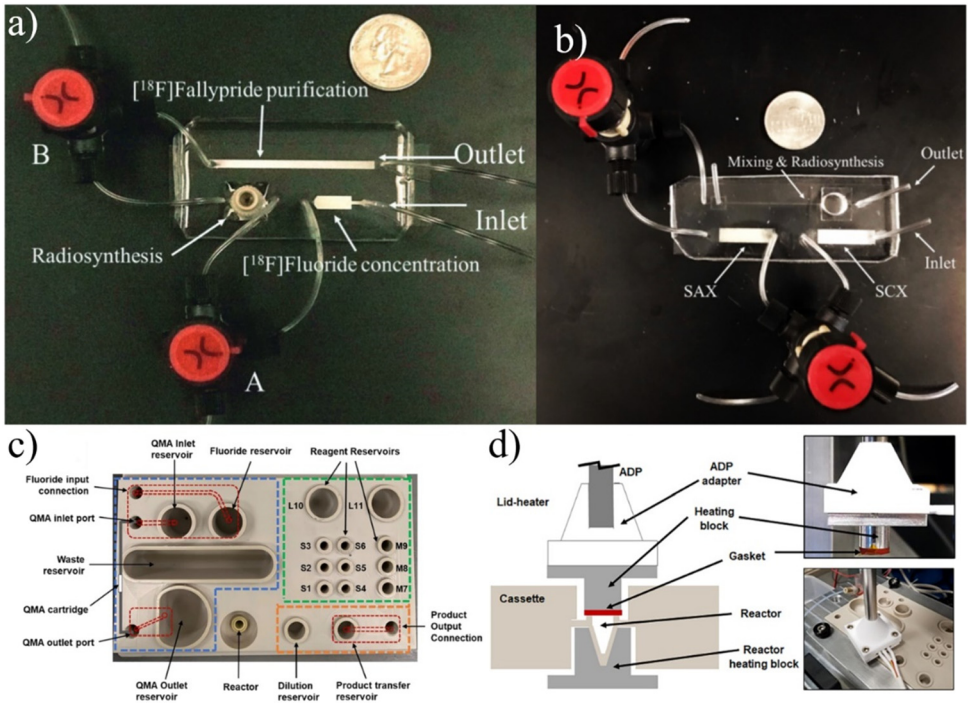

Fig. 7 a) RAPID-F[90] and b)RAPID-M[91] devices contain on-chip SPE columns so that no external processing is required and the chips can be packaged into an extremely compact synthesis module. c and d) PHENYX approaches batch synthesis different utilizing open-air chambers and robotic pipetting to eliminate macro-to-microfluidic interfacing.[98] Used with permission of a and b) Royal Society of Chemistry from ref. 90 and 91, and b) Elsevier from ref. 98; permission conveyed through Copyright Clearance Center, Inc.

volume to below 20 μL while maintaining the desired concentrations by introducing a secondary ion exchange step and an optimal evaporation procedure. The refined pre-reaction procedure allowed them to synthesize a range of ^{18}F-labeled radiotracers with RCYs comparable to other microfluidic reports.[92] Additional work was done to calibrate reactions of [^{18}F]FET and [^{18}F]fallypride to achieve substantial radiochemical yield at volumes less than 20 μL.[97] Unlike more conventional microfluidic platforms described in this review, this design focuses on achieving microvolume reactions using already established equipment. In fact, they have fully integrated their concentration techniques and microreactor directly into GE's FASTlab module, achieving high RCY and reducing reagent volumes by 80–90%.[97] However, directly integrating a microscale reactor into current commercially available equipment would not achieve the complete shift to decentralized radiotracer production. Still, the group is developing their own automation module that could be used for production while avoiding some of the complications of microfluidics such as the macro-to-micro fluidic interface.

Lu *et al.* have recently reported a unique platform named PHENYX that is centered around a disposable cassette with a 50 μL open-air reactor.[98] The cassette is machined from PEEK and contains regions for concentration, labeling, and dilution (Fig. 7c and d). Fluid is transported throughout the chip either by robotic top-down pipetting or *via* machined microfluidic channels. Fluid flow through the channels is driven by sealing and pressurizing the exposed reservoirs. The cassette contains an SPE cartridge that is used to concentrate the raw material. The reaction is completed in a heated on-chip vial that is robotically covered by a heated lid. The product is diluted *via* pipetting and must be moved off-chip for further purification.

Highly integrated/automated solutions

ISAR. Frank *et al.* first reported on a fully automated radiotracer production platform named ISAR in 2018.[99] The synthesis module works around a multi-layered cyclic olefin copolymer (COC) microfluidic device (Fig. 8a) that contains 70 membrane valves and numerous channels to provide pathways between 70 external Luer connections and two on-chip reaction chambers (Fig. 8b). The chips are designed so that reactions can be run in parallel, allowing the system to achieve production of multiple different tracers using the same chip. The Luer connections provide a way to seamlessly integrate standard laboratory items such as ion exchange columns as the microfluidic chip does not contain such components.

The membrane valves are controlled *via* an electro-pneumatically actuated plunger which provides extremely accurate metering for both liquid and gas phase reactions.[99] Macro-to-micro fluidic interfacing is a significant problem for commercial microfluidic platforms and the valve-Luer connection scheme of ISAR establishes an elegant solution. However, this solution also requires manual loading of the different Luer-connected components for specific synthesis

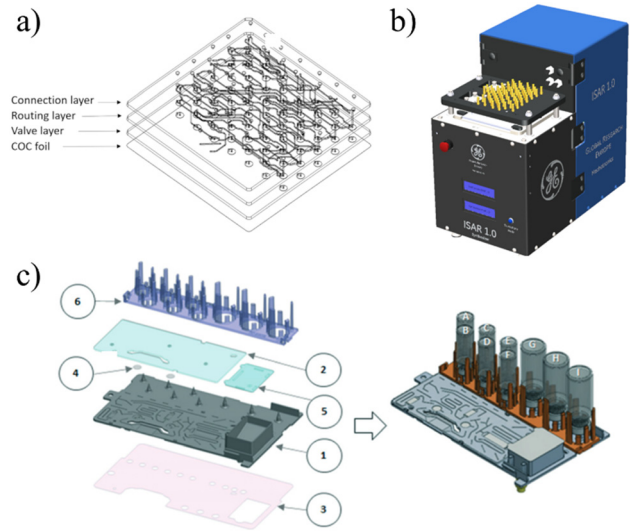

Fig. 8 The ISAR platform is built around a) a COC microfluidic chip that is controlled by b) a fully automated unit that uses Luer connections to direct fluid and interface with macrofluidic components (SPE columns, *etc.*) as needed.[99] c) iMiDEV is a fully automated module built around a multilayered microfluidic device that uses externally attached vials of reagents and microfluidic valves to execute radiosyntheses entirely on-chip.[102] Used with permission of a and b) Springer Nature from ref. 99, and c) Royal Society of Chemistry from ref. 102; permission conveyed through Copyright Clearance Center, Inc.

runs which decreases the overall automation and increases the risk of human error. The system requires a hot-cell, and for each type of synthesis a unique chip must be designed and fabricated (which increases cost). ISAR has been validated multiple times, producing quality [^{18}F]FDG, [^{13}N]NH_3, and [^{68}Ga]PSMA.[99,100]

iMiLAB/iMiDEV™. A highly integrated batch-based platform called iMiLAB® has been developed by iMiGiNE, a medical systems subsidiary of PMB Alcen in France. The production platform and its R&D counterpart iMiDEV™ operate using a microfluidic cassette-like chip (Fig. 8c). The platform leverages fully automated chip loading and fluidic interfacing to minimize human interaction. The chip contains a single liquid phase reactor and three solid phase columns that can be accessed at the operator's command *via* 34 pneumatically actuated microfluidic valves.[101] It also contains a series of vial connections on which preloaded vials of reagents are loaded. iMiDEV™ has been used to produce [^{18}F]NaF in a fully automated fashion in only 8 min with a RCY of 82%.[102] It was also shown to automatically synthesize quality ^{11}C and ^{68}Ga radiotracers.[101,103,104] This platform represents a major milestone as one of the few fully integrated and customizable microfluidic platforms for radiotracer synthesis.

Users have, however, reported substantial variability in fluidic resistance between batches which strongly affects the overall yield of the system.[103] Still, the iMiDEV™ system has set a new standard for the industry with its unprecedented level of integration, automation, and customization.

Droplet

Early research and development. In 2011, Liu *et al.* developed a droplet device with the intention of minimizing the reaction volume of syntheses for radiotracer developmental purposes.[108] Specifically, it was designed to vary the pH and precursor concentration for the synthesis of [^{18}F]FB-A2 Db. The volume of each reaction was only 40 nL, allowing users to efficiently iterate through reaction conditions that can then be used to scale up to dose-level optimization. This design was complex, with multiple on-chip valves and operated at volumes (and corresponding activities) too small for any clear path to human dose production. The field then shifted to electrowetting-on-dielectric (EWOD) devices which maintained microvolumes while also introducing fully programmable fluid flow paths. The van Dam group developed the first EWOD chips specifically for radiotracer synthesis on a glass substrate using layers of ITO, dielectric, and the hydrophobic material Cytop® (Fig. 9a).[105] The authors were able to efficiently synthesize at volumes no more than 17 μL. This platform was further developed to drastically increase capability, reliability, and level of automation (Fig. 9b and c).[95,96,106,109–112]

There has also been a limited amount of research into using magnetism to drive the transport of droplets across chips. Fiel *et al.* reported on this design strategy wherein magnetic particles that are chemically activated act as both the carrier of reagents and ion exchange resin.[107] Using a magnet on a movable stage below, particles are moved across a Teflon sheet to collect, transport, and mix small volumes of liquid *via* surface tension (Fig. 9d). The platform is a unique application of droplet-based microfluidics but has not been developed further due to progress in simpler droplet devices with reduced fabrication costs and increased reliability.[109]

Recent/active development. Although EWOD chips could reliably produce high quality radiotracers with minimal reagents, they were hindered by complexity and cost.[109] The concept of droplet radiochemistry was still promising, so focus has since shifted to passive transport wherein droplets on a silicon chip are controlled based on the geometry of a patterned hydrophilic surface. Originally, a star-like design was used to transport droplets from loading sites to a central reaction site (Fig. 10a).[113] The design was amenable to automation and integration with other operations (*e.g.* concentration), as droplets could to be dispensed onto the chip without direct contact, eliminating the need for fluidic interfacing of tubing.[114] This design has been further simplified to just a circular area of hydrophilic silicon (Fig. 10b) to which any necessary reagents can be added *via* an automated dispenser (Fig. 10c).[115] The platform has been actively developed in the past few years with large focus on automation and robustness such that it can perform a wide array of syntheses including single to multi-dose quantities of [^{18}F]fallypride, [^{18}F]FET, [^{18}F]florbetaben.[114,116–121]

Highly integrated/automated solutions. The passively held droplet chip developed by the van Dam group has recently

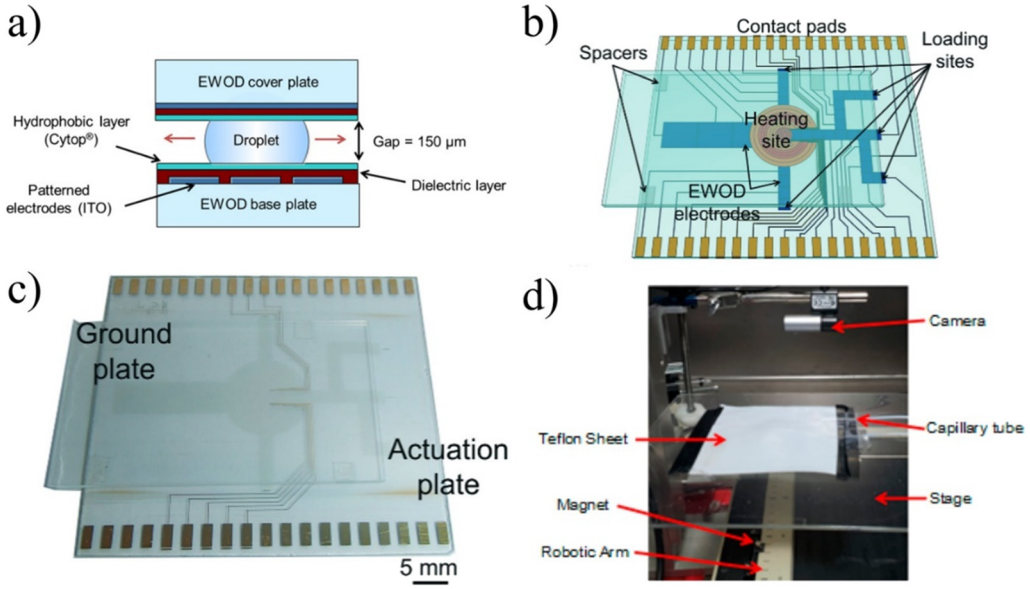

Fig. 9 a) EWOD devices function by compressing droplets on top of patterned electrodes and as different electrodes are activated, the droplet moves along the electrodes, allowing for complete control of the droplet.[105] Copyright 2012 National Academy of Sciences. b and c) To automatically and reliably synthesize complex radiotracers, the design included loading sites on which different reagents could be dropped and a heated reaction site to conduct radiolabeling. Used with permission of Royal Society of Chemistry from ref. 106; permission conveyed through Copyright Clearance Center, Inc. d) Magnetically controlled droplets for radiotracer synthesis was a novel implementation, but has not shown the ability to execute elevated temperature reactions or operate with various organic solvents. Reprinted with permission from ref. 107. Copyright 2015 American Chemical Society.

been automated with a focus on radiotracer research and development. Jones *et al.* have described a fully automated platform that can screen up to 64 reaction conditions in a single run (Fig. 11).[122] The platform centers around four chips, each containing 16 droplet reaction sites. Fluid is handled *via* a fluidics head attached to an *X*–*Y*–*Z* gantry that traverses the machine. The fluidics head contains seven piezoelectric dispensers and a single pipette port. The dispensers are permanently connected to vials of reagents that are common to multiple reactions. A pipette, fed by a syringe pump and loaded with tips from a tip rack, handles reaction-specific solution deposition as well as collection of fluid off the chip. Finally, the platform contains a thin-layer chromatography (TLC) plate holder used to determine fluorination efficiency.[123,124] Although it does not directly address the issue of full scale radiotracer production, the platform is revolutionary for its ability to rapidly iterate through such a high number of conditions with a very small volume of reagents and precursors, and achieves results commensurate with full scale optimization experiments.[122]

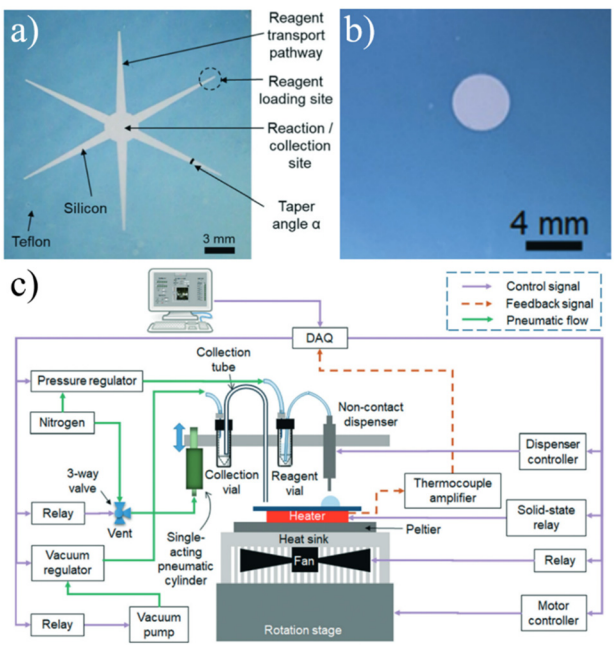

Fig. 10 a) The original passively-held droplet design used a star-like shape to create transport channels for reagents to collect into a single reaction site.[113] b) Later iterations eliminated the channels in favor of dispensing the various reagents directly onto the reactions site using c) an automated microdropping system.[116] Used with permission of Royal Society of Chemistry from ref. 113 and 116; permission conveyed through Copyright Clearance Center, Inc.

Practical considerations for commercial platforms

The majority of research and development in this field has been rightfully focused on developing robust microfluidic devices for radiotracer synthesis. To transition these impressive research projects to widespread commercial use, all the logistical aspects of operation must be considered (Table 1). These considerations will be discussed in the framework of being either financial or regulatory obligations.

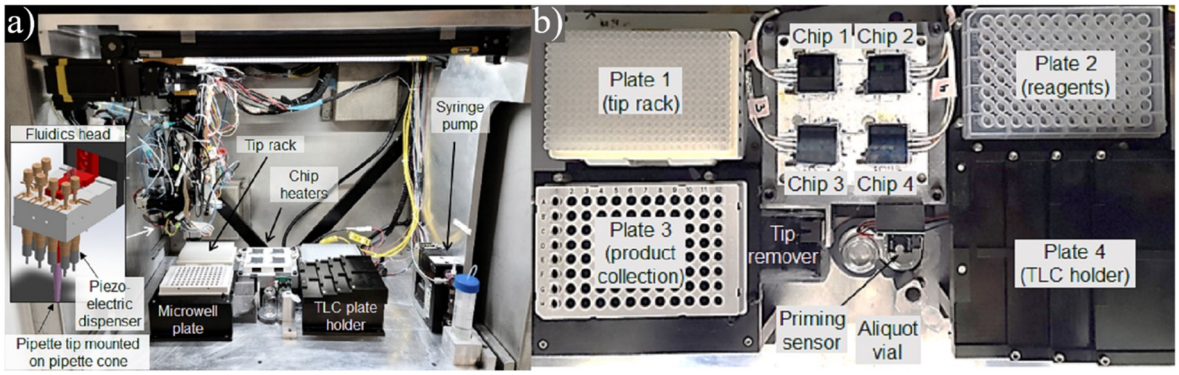

Fig. 11 a) Centered around 64 passively held droplet reaction sites, this platform allows researchers to rapidly iterate through expansive parameter spaces with little human interaction. b) The unit contains all the necessary components for automation and a section for TLC analysis to quantify the results. Used with permission of Elsevier Science & Technology Journals from ref. 122; permission conveyed through Copyright Clearance Center, Inc.

Financial considerations

At its core, microfluidic production of radiotracers is a solution to a cost problem. Production facilities have the capability to synthesize boutique tracers, but it is not profitable for them to do so. The leading drivers of cost are 1) equipment designed for large batch production, 2) large and expensive auxiliary equipment (*i.e.* hot cells), and 3) highly skilled and dedicated operators. Microfluidic production could fundamentally eliminate the first problem, and so the engineering to implement these new approaches must account for the latter two issues. The most direct way to accomplish these is to design a completely automated platform that can be operated outside of a hot cell. Moreover, developers must choose appropriate materials for the microfluidic devices to ensure high RCY and low manufacturing costs.

Shielding. Properly shielding all radioactive material is of utmost importance for the safety of all individuals nearby. Commercial systems must be operated within the confines of a hot cell, which are large and expensive. Microfluidic systems can be integrated into a benchtop platform containing all necessary shielding thereby eliminating the need for hot cells. A commercialized example of this was the Modular-Lab MicroCell (Eckert & Ziegler) in which the synthesis cassette was designed to fit into a benchtop lead box and could be controlled externally. Solutions like this allow the end user (hospitals, scanning centers, *etc.*) to implement the module into their facility with little-to-no additional materials. Indeed, the cost, maintenance, and space requirements of hot cell installation would likely be a dealbreaker for most scanning facilities so it is critical that a well-developed platform can be safely operated outside of one.

A promising solution to this would be that of a "split-box" design as spearheaded by Lebedev *et al.*[88] where all operations that employ activity are within a shielded area, and everything else is outside of it. This is an attractive design as it minimizes the amount of shielding needed and allows external access to precursors and other reagents. Implementation of this design must be done carefully to ensure internal-to-external connections (*i.e.* tubing and wiring) do not release radiation to the surroundings.

Automation/integration. For microfluidic radiosynthesis to completely flip the radiotracer supply chain, it is critical that the final system can autonomously produce a ready-to-use human dose from the raw product of cyclotrons and generators. A large part of the cost of radiotracer production comes from the highly trained operators that are necessary to operate commercial equipment. It is imperative that microfluidic platforms reduce this cost by attaining a level of automation and integration such that the operator has little-to-no interaction with the machine beyond very simple preparation or maintenance. Achieving this will require complete integration of all steps of radiosynthesis such that no external components (*i.e.* SPE cartridges) need manual replacement between each run. Additionally, automation enables complete programmatic control for things like fluid pathways, reaction temperature, and flowrates. This would not only minimize operator interaction but also maximize the flexibility and reproducibility of the system, and additionally ensure that it can produce novel radiotracers developed in the future. The system must be able to rapidly execute a cleaning cycle to ensure there is no cross contamination. This will come through a combination of flushing lines and discarding single-use components. An efficient cleaning cycle helps ensure high throughput, which is critical for systems that would be producing multiple different doses of different radiotracers in a single day.

Materials. Choosing a material to use when fabricating microfluidic devices is a complex task and developers must consider several parameters including cost of material, cost/

Table 1 Comparison of the key aspects discussed of some commercialized and in-development microfluidic platforms

Platform	Reactor type	Concentration/ solvent switching	Radiolabeling/ deprotection	Purification/ reformulation	Automated fluidic handling	Level of operator interaction	Shielding	Activity tracking
iMiLAB/iMiDEV[102]	Batch	On-chip	On-chip	On-chip	Gas pressure driven	Load reagents for each chip	Hot-cell	PIN diodes
ISAR[99]	Batch	Externally attached	On-chip	Integrated external unit	Gas pressure driven	Attaching and replacing external components	Hot-cell	Not reported
RAPID[90,91]	Batch	On-chip	On-chip	On-chip	Not yet demonstrated	Fluidic handling	Hot-cell	Not reported
Lisova *et al.*[117]	Droplet	Integrated external unit	On-chip	Integrated external unit	Gas pressure driven	Manual transfer to HPLC/purification	Hot-cell	Ion chamber

ease of fabrication, and chemical compatibility. The microfluidic devices reported herein have been fabricated using a wide range of materials including polydimethylsiloxane (PDMS),[86,90,91] cyclic olefin polymers/ copolymer (COP/C),[99,102] polyether ether ketone (PEEK),[98] and silicon (used as a substrate for droplet reactions).[117,122]

PDMS has long been a material of debate for radiotracer devices. It is a highly attractive material for its low cost, ease of fabrication, optical transparency, and the vast knowledge base concerning its use for microfluidics.[125] For these reasons, PDMS was used for early devices but researchers suspected there was significant interaction between ^{18}F and PDMS that would cause reductions in radiochemical yield, and reported losses as high as 90%.[38,86,126,127] These losses would be detrimental to the economic viability of any commercial platform and so in 2010, Tseng *et al.* conducted a study examining the interaction of ^{18}F and PDMS during the drying/evaporation step.[128] A solution of ^{18}F and MeCN in a serpentine microfluidic channel was evaporated through a thin membrane at 105 °C. By imaging the Cherenkov radiation, activity was measured both before and after evaporation and indicated that losses were under 10%. Additional heating beyond the point of complete solvent evaporation resulted in significant losses, demonstrating that interaction with PDMS is likely a strong function of temperature and time. Control experiments during which no heat was applied after evaporation for the same period showed negligible loss. The authors suggested the loss could be attributed to a direct reaction with ^{18}F under heat and to an integration of ^{18}F into the PDMS structure. More recently in 2019, Fernandez-Maza *et al.* completed another study on this interaction in which 30 μL of ^{18}F and MeCN with varying amounts of activity were evaporated from a reaction chamber.[129] Activity in the chamber was measured thrice for each trial: before and after evaporation and after water elution. The activity of the elution water was also measured. Results from these trials concluded that there was little to no interaction between ^{18}F and PDMS with negligible activity remaining on-chip after elution (two water elutions were used for 4 of the 8 trials). The authors suggested that possible disagreement in data could be attributed to differing surface roughness where higher roughness would induce more absorption.

Overall, the field has shifted away from the use of PDMS in favor of materials less likely to interact with ^{18}F, namely COP/COC's, PEEK, and silicon. COP/COC's are highly inert and stable polymers and are economical when mass produced through molding but can be very costly to use when prototyping designs.[125] PEEK is also highly inert but is expensive, optically opaque, and requires either machining or injection molding for complex fabrication,[98] rendering it a rather difficult material for prototyping as well. Some devices have been made with silicon as a substrate for droplet-based reactors.[117,122] If direct interaction with the radionuclide can be limited, PDMS (potentially enhanced by inert coatings) still holds potential as a cheap and easily employed prototyping material, but COP/COC's and PEEK have emerged as the standout materials for mass production of microfluidic devices for radiotracer synthesis.

Safety and regulatory considerations

For a microfluidic platform to be commercially viable, it must adhere to standards and protocols that ensure the safety of the operators and patients. These considerations include, but are not limited to, shielding (discussed earlier), activity tracking during synthesis, and proper QC.

Activity tracking. It is critical that any commercial platform has a robust activity tracking system in place. Researchers integrating activity tracking into microfluidic platforms have implemented a number of different techniques including Cherenkov radiation imaging, photomultipliers, and scintillation-based sensors.

Cherenkov radiation occurs when a particle moves in a medium faster than the phase velocity of light in that medium.[130] When ^{18}F decays and releases a positron, the particle can briefly achieve velocities high enough to create Cherenkov radiation which can propagate and produce a spectrum from the near-UV to visible spectrum.[131] The radiation has been used to image radiation through PDMS,[128,132] glass,[96,105,114–116] and a plastic scintillator.[116] However, imaging with Cherenkov radiation (and phosphor

plates, an imaging technique used in several papers[133–135]) is a discrete detection method and therefore cannot be implemented as a continuous measurement technique. The topic of employing Cherenkov radiation imaging for microfluidic radiotracer production was recently covered in a review by van Dam and Chatziioannou.[136] Another effective method has been to use silicon photomultiplier (SiPM) chips that yield reliable detection based off direct interaction with beta particles.[137–140] However, this interaction requires that the detector is very close to the microfluidic channel, which may not be possible for some designs. Scintillators have been used as an intermediate material to enhance the signal from positron interactions,[141] and as a standalone detection device.[142–144] Silicon sensors have also been explored as a detection mechanism.[140,145]

Quality control. The microfluidic platforms described above have almost exclusively considered the production aspects of radiotracer synthesis. To adhere to current good manufacturing practice (cGMP) regulations, the doses formulated must undergo rigorous QC before being used in humans. As mentioned above, radiotracers must pass tests for appearance, radionuclide and radiochemical identity, bacterial endotoxins, pH, radiochemical, radionuclide, and chemical purity, residual solvents, and sterility.[25] Traditional QC methods are costly as they require a range of tests across multiple analytical instruments including a radio-HPLC, gas chromatograph, dose calibrator, and others.[117,146]

A well-developed QC platform fully integrated with a microfluidic synthesis module is critical to the goal of decentralized radiotracer production. This would allow a technician to simply load the raw radioactive material and relevant precursors and solvents, start the machine, and receive a fully qualified human-ready dose of tracer without any further interaction. Elizarov has written an extensive chapter detailing the history and progress made of QC regulations and commercial equipment.[146]

In 2017, Trace-Ability, Inc. released the Tracer-QC which revolutionized QC of radiotracers by generating all necessary validation data from measurements produced by a plate reader. Because it includes an integrated HPLC, this methodology eliminates the need for several different bulky machines. An additional benefit to this platform is that it can be fully shielded without a hot cell. The platform also receives the radiotracer insulated in a pig (a small lead-shielded container),[146] thus eliminating any direct exposure of the operator to radioactive material. The system requires minimal setup by providing prepackaged kits; afterward all steps are automated. This not only reduces the training requirements for operators but also allows them to tend to other tasks while the machine is operating and may improve reproducibility. Indeed, the Tracer-QC has already been used to validate radiotracers synthesized by microfluidics.[117]

The German company QC1 GmbH was established to create a standalone, fully automated QC unit for radiotracers. As opposed to the Tracer-QC which fundamentally changed the way it was collecting QC metrics, the QC1 was designed as an ultra-compact automated version of all necessary traditional equipment.[146] In 2018, Trasis took over the platform and has developed it to the point of commercial release in 2023. The current platform uses a design in which kits that contain various components required for the QC are placed into two slots in the machine. The operator then selects what tracer is being tested and the platform will conduct all tests in roughly 30 minutes.[147] Although it is not a standalone QC unit, the BG-75 Biomarker Generator (Best ABT Molecular Imaging) has a fully incorporated QC module which validates the idea of integrating automated synthesis and QC. Both the Tracer-QC and QC1 are extremely promising platforms that could provide full QC services by integrating with future commercial microfluidic synthesis platform.

Although these platforms have fundamentally changed the way QC can be completed, several research groups continue to dedicate efforts towards developing true microfluidic QC devices. In 2018, Ly *et al.* developed a microfluidic chip that was designed to replace an HPLC for radiochemical identity and purity tests by using microchip electrophoresis (MCE).[148] This technique used two chips, an injection and a detection chip, connected by a capillary tube. In the injection chip, the sample was loaded, and an electric potential was applied across the length of the capillary tube to the detection chip. The applied potential caused different chemical species to traverse the length of the capillary tube at different rates. In the detection chip, the absorbance of the fluid at a characteristic wavelength was measured to detect the presence of a chemical species. The time it took for the compound to travel the length of the capillary tube was compared to that of a standard solution which was used to confirm the identity of the species. This method was shown to provide results comparable to HPLC while reducing the required volume of radiotracer to the order of nanoliters.

In 2020, Patinglag *et al.* developed both single-use and multiple-use microfluidic devices that also focused on satisfying the radiochemical identity and purity portion of QC for [^{18}F]FDG. This was accomplished by combining ion exchange chromatography, radiation detection and a technique called pulsed amperometric detection. As [^{18}F]FDG was separated in the ion exchange column, a potential was applied across the eluent and the change in current was measured as the glucose analog was oxidized. The time of peak current was used to identify the species (in comparison to a standard solution) and the amount of current can be used to determine concentration.[149] While these results are exciting, significant research is still needed to achieve a microfluidic device capable of satisfying all QC metrics. Reducing QC apparatus to a single microfluidic platform could help to further reduce the time, space, and cost requirements of other methods, which would further expedite the transition to decentralized radiotracer production.

Conclusions

Since the development of PET over 40 years ago, the industry has been dominated by a single radiotracer, [^{18}F]FDG. Although the glucose analog has been instrumental to millions of diagnoses, PET holds incredible potential to track any biological process of interest if the correct radiotracer is chosen. To this end, there have been thousands of novel radiotracers developed in laboratories that never reach the stage of clinical use. A major reason for this is the overbearing cost of radiotracer production. As centralized facilities produce both the radionuclides and the radiotracers in large batches to capitalize on economies of scale, economic production of boutique tracers is impossible. To address this issue, many researchers have sought to develop microfluidic devices that could facilitate the shift from current production approaches to a dose-on-demand concept. In this concept, centralized production centers would distribute radionuclides to local scanning sites and there, using an in-house microfluidic system, various radiotracers would be synthesized as needed. This review aimed to provide a broad overview of the history and current progress towards microfluidic synthesis of radiotracers and decentralized production. Successful implementation of one or multiple of these platforms will enable precision medicine and invigorate radiochemists to develop additional radiotracers with the knowledge that physicians will be able to harness them.

The radiotracer production process can be thought of as three steps – 1) radionuclide production, 2) radiotracer synthesis, and 3) QC. Radionuclide production is a well-established field and continual developments have reduced the cost and difficulty of this process.[150] This leaves synthesis and QC to be developed for on-site dose-on-demand production. QC has historically been a more cumbersome task requiring vast amounts of equipment, space, and personnel. However, with the recent introduction of fully automated modules such as the Tracer-QC and QC1, this task has been drastically simplified to effectively pressing "START" on a benchtop machine. This leaves one piece of the puzzle missing – radiotracer synthesis. To push PET forward as a precision medicine tool, it is imperative to create a compact, benchtop platform that can rapidly and autonomously produce a wide array of radiotracers.

The field of microfluidic radiotracer synthesis has been in development for nearly 20 years and has advanced to a point that it is now time to focus efforts on transitioning the technology from the lab to commercial settings. Assuming the core microfluidic device capable of various radiochemical syntheses has been developed (as has been shown by multiple projects in this review), the critical considerations for commercial viability are:

Automation: limit interaction to, at most, simple reagent preparation and process activation.

Flexibility: produce many different tracers with no additional preparation.

Throughput: produce multiple doses of radiotracers in a single day.

Cost and size: bench top platform with cheap consumables.

Microfluidic radiotracer synthesis platforms are on the brink of commercialization. By approaching future development with a strong engineering focus on logistically simple and economically viable systems, dose-on-demand synthesis could soon upend the radiotracer pipeline and allow the medical field to unleash the full power of personalized nuclear medicine.

Author contributions

The original draft was written by MM. The manuscript was reviewed and edited by MM and LMB.

Conflicts of interest

There are no conflicts to declare.

Acknowledgements

Fig. 1 and 2 created with **https://BioRender.com**.

References

1 L. H. Portnow, D. E. Vaillancourt and M. S. Okun, *Neurology*, 2013, **80**, 952–956.
2 L. I. Wiebe, *Radiat. Phys. Chem.*, 1984, **24**, 365–372.
3 C. Rensch, B. Waengler, A. Yaroshenko, V. Samper, M. Baller, N. Heumesser, J. Ulin, S. Riese and G. Reischl, *Appl. Radiat. Isot.*, 2012, **70**, 1691–1697.
4 R. N. Krasikova, *Radiochemistry*, 2023, **65**, 158–176.
5 N. R. C. (US) and I. of M. (US) C. on the M. and P. of E. D. B. Imaging, in *Mathematics and Physics of Emerging Biomedical Imaging*, National Academies Press (US), 1996.
6 M. Lin, R. P. Coll, A. S. Cohen, D. K. Georgiou and H. C. Manning, *Molecules*, 2022, **27**, 6790.
7 OECD Statistics, **https://stats.oecd.org/Index.aspx?ThemeTreeId=9**, (accessed August 3, 2023).
8 S. Y. Park, C. Mosci, M. Kumar, M. Wardak, N. Koglin, S. Bullich, A. Mueller, M. Berndt, A. W. Stephens, F. T. Chin, S. S. Gambhir and E. S. Mittra, *EJNMMI Res.*, 2020, **10**, 100.
9 D. Petroni, L. Menichetti and M. Poli, *J. Radioanal. Nucl. Chem.*, 2020, **323**, 1017–1031.
10 M. V. Liberti and J. W. Locasale, *Trends Biochem. Sci.*, 2016, **41**, 211–218.
11 J. M. Hooker and R. E. Carson, *Annu. Rev. Biomed. Eng.*, 2019, **21**, 551–581.
12 A. Leuzy, I. Savitcheva, K. Chiotis, J. Lilja, P. Andersen, N. Bogdanovic, V. Jelic and A. Nordberg, *Eur. J. Nucl. Med. Mol. Imaging*, 2019, **46**, 1276–1286.
13 I. M. Jackson, S. J. Lee, A. R. Sowa, M. E. Rodnick, L. Bruton, M. Clark, S. Preshlock, J. Rothley, V. E. Rogers, L. E. Botti, B. D. Henderson, B. G. Hockley, J. Torres, D. M. Raffel, A. F. Brooks, K. A. Frey, M. R. Kilbourn, R. A.

Koeppe, X. Shao and P. J. H. Scott, *EJNMMI Radiopharm. Chem.*, 2020, **5**, 24.
14 N. A. Gharibkandi and S. J. Hosseinimehr, *Eur. J. Med. Chem.*, 2019, **166**, 75–89.
15 K.-A. Knapp, M. L. Nickels and H. C. Manning, *Mol. Imaging Biol.*, 2020, **22**, 463–475.
16 C. Barca, C. M. Griessinger, A. Faust, D. Depke, M. Essler, A. D. Windhorst, N. Devoogdt, K. M. Brindle, M. Schäfers, B. Zinnhardt and A. H. Jacobs, *Pharmaceuticals*, 2021, **15**, 13.
17 K. Herrmann, M. Schwaiger, J. S. Lewis, S. B. Solomon, B. J. McNeil, M. Baumann, S. S. Gambhir, H. Hricak and R. Weissleder, *Lancet Oncol.*, 2020, **21**, e146–e156.
18 S. B. Hansen, *Semin. Nucl. Med.*, 2022, **52**, 266–275.
19 O. Jacobson, D. O. Kiesewetter and X. Chen, *Bioconjugate Chem.*, 2015, **26**, 1–18.
20 S. S. Gambhir, *Nat. Rev. Cancer*, 2002, **2**, 683–693.
21 C. Rensch, A. Jackson, S. Lindner, R. Salvamoser, V. Samper, S. Riese, P. Bartenstein, C. Wängler and B. Wängler, *Molecules*, 2013, **18**, 7930–7956.
22 H. Elkawad, Y. Xu, M. Tian, C. Jin, H. Zhang, K. Yu and Q. He, *Chem. – Asian J.*, 2022, **17**, e202200579.
23 N. S. Ha, S. Sadeghi and R. M. VanDam, *Micromachines*, 2017, **8**, 337.
24 H. H. Coenen, A. D. Gee, M. Adam, G. Antoni, C. S. Cutler, Y. Fujibayashi, J. M. Jeong, R. H. Mach, T. L. Mindt, V. W. Pike and A. D. Windhorst, *Ann. Nucl. Med.*, 2018, **32**, 236–238.
25 United States Pharmacopeia, *USP Monographs, Fludeoxyglucose F 18 Injection*, USP-NF, United States Pharmacopeia, Rockville, MD, 2023.
26 P. Y. Keng, M. Esterby, R. M. van Dam, P. Y. Keng, M. Esterby and R. M. van Dam, in *Positron Emission Tomography – Current Clinical and Research Aspects*, IntechOpen, 2012.
27 D. Zeng, A. V. Desai, D. Ranganathan, T. D. Wheeler, P. J. A. Kenis and D. E. Reichert, *Nucl. Med. Biol.*, 2013, **40**, 42–51.
28 B. Zhang, B. H. Fraser, M. A. Klenner, Z. Chen, S. H. Liang, M. Massi, A. J. Robinson and G. Pascali, *Chem. – Eur. J.*, 2019, **25**, 7613–7617.
29 G. Pascali, P. Watts and P. A. Salvadori, *Nucl. Med. Biol.*, 2013, **40**, 776–787.
30 S.-Y. Lu, P. Watts, F. T. Chin, J. Hong, J. L. Musachio, E. Briard and V. W. Pike, *Lab Chip*, 2004, **4**, 523–525.
31 J. M. Gillies, C. Prenant, G. N. Chimon, G. J. Smethurst, W. Perrie, I. Hamblett, B. Dekker and J. Zweit, *Appl. Radiat. Isot.*, 2006, **64**, 325–332.
32 J. M. Gillies, C. Prenant, G. N. Chimon, G. J. Smethurst, B. A. Dekker and J. Zweit, *Appl. Radiat. Isot.*, 2006, **64**, 333–336.
33 P. W. Miller, N. J. Long, A. J. de Mello, R. Vilar, H. Audrain, D. Bender, J. Passchier and A. Gee, *Angew. Chem.*, 2007, **119**, 2933–2936.
34 P. W. Miller, H. Audrain, D. Bender, A. J. deMello, A. D. Gee, N. J. Long and R. Vilar, *Chem. – Eur. J.*, 2011, **17**, 460–463.
35 C. J. Steel, A. T. O'Brien, S. K. Luthra and F. Brady, *J. Labelled Compd. Radiopharm.*, 2007, **50**, 308–311.
36 H.-J. Wester, B. W. Schoultz, C. Hultsch and G. Henriksen, *Eur. J. Nucl. Med. Mol. Imaging*, 2009, **36**, 653–658.
37 T. D. Wheeler, D. Zeng, A. V. Desai, B. Önal, D. E. Reichert and P. J. A. Kenis, *Lab Chip*, 2010, **10**, 3387–3396.
38 S. Haroun, Z. Sanei, S. Jivan, P. Schaffer, T. J. Ruth and P. C. H. Li, *Can. J. Chem.*, 2013, **91**, 326–332.
39 R. Ismail, J. Irribaren, M. R. Javed, A. Machness, R. M. van Dam and P. Y. Keng, *RSC Adv.*, 2014, **4**, 25348–25356.
40 H. Kawashima, H. Kimura, Y. Nakaya, K. Tomatsu, K. Arimitsu, H. Nakanishi, E. Ozeki, Y. Kuge and H. Saji, *Chem. Pharm. Bull.*, 2015, **63**, 737–740.
41 H. Kimura, K. Tomatsu, H. Saiki, K. Arimitsu, M. Ono, H. Kawashima, R. Iwata, H. Nakanishi, E. Ozeki, Y. Kuge and H. Saji, *PLoS One*, 2016, **11**, e0159303.
42 W.-Y. Tseng and R. M. van Dam, *Lab Chip*, 2014, **14**, 2293–2302.
43 B. Z. Cvetković, O. Lade, L. Marra, V. Arima, R. Rinaldi and P. S. Dittrich, *RSC Adv.*, 2012, **2**, 11117–11122.
44 V. Arima, G. Pascali, O. Lade, H. R. Kretschmer, I. Bernsdorf, V. Hammond, P. Watts, F. D. Leonardis, M. D. Tarn, N. Pamme, B. Z. Cvetkovic, P. S. Dittrich, N. Vasovic, R. Duane, A. Jaksic, A. Zacheo, A. Zizzari, L. Marra, E. Perrone, P. A. Salvadori and R. Rinaldi, *Lab Chip*, 2013, **13**, 2328–2336.
45 F. De Leonardis, G. Pascali, P. A. Salvadori, P. Watts and N. Pamme, *J. Chromatogr. A*, 2011, **1218**, 4714–4719.
46 M. D. Tarn, G. Pascali, F. De Leonardis, P. Watts, P. A. Salvadori and N. Pamme, *J. Chromatogr. A*, 2013, **1280**, 117–121.
47 G. Pascali, G. Mazzone, G. Saccomanni, C. Manera and P. A. Salvadori, *Nucl. Med. Biol.*, 2010, **37**, 547–555.
48 G. Pascali, A. Berton, M. DeSimone, N. Wyatt, L. Matesic, I. Greguric and P. A. Salvadori, *Appl. Radiat. Isot.*, 2014, **84**, 40–47.
49 S. Lu, A. M. Giamis and V. W. Pike, *Curr. Radiopharm.*, 2009, **2**, 49–55.
50 H. Anderson, N. Pillarsetty, M. Cantorias and J. S. Lewis, *Nucl. Med. Biol.*, 2010, **37**, 439–442.
51 S. Lu and V. W. Pike, *J. Fluorine Chem.*, 2010, **131**, 1032–1038.
52 V. R. Bouvet, M. Wuest, L. I. Wiebe and F. Wuest, *Nucl. Med. Biol.*, 2011, **38**, 235–245.
53 J. Ungersboeck, C. Philippe, L.-K. Mien, D. Haeusler, K. Shanab, R. Lanzenberger, H. Spreitzer, B. K. Keppler, R. Dudczak, K. Kletter, M. Mitterhauser and W. Wadsak, *Nucl. Med. Biol.*, 2011, **38**, 427–434.
54 S. Kealey, C. Plisson, T. L. Collier, N. J. Long, S. M. Husbands, L. Martarello and A. D. Gee, *Org. Biomol. Chem.*, 2011, **9**, 3313–3319.
55 G. Pascali, G. Nannavecchia, S. Pitzianti and P. A. Salvadori, *Nucl. Med. Biol.*, 2011, **38**, 637–644.
56 J.-H. Chun, S. Lu and V. W. Pike, *Eur. J. Org. Chem.*, 2011, **2011**, 4439–4447.

57 S. Telu, J.-H. Chun, F. G. Siméon, S. Lu and V. W. Pike, *Org. Biomol. Chem.*, 2011, **9**, 6629–6638.
58 K. Dahl, M. Schou and C. Halldin, *J. Labelled Compd. Radiopharm.*, 2012, **55**, 455–459.
59 R. W. Simms, P. W. Causey, D. M. Weaver, C. Sundararajan, K. A. Stephenson and J. F. Valliant, *J. Labelled Compd. Radiopharm.*, 2012, **55**, 18–22.
60 V. Bouvet, M. Wuest, P.-H. Tam, M. Wang and F. Wuest, *Bioorg. Med. Chem. Lett.*, 2012, **22**, 2291–2295.
61 S. V. Selivanova, L. Mu, J. Ungersboeck, T. Stellfeld, S. M. Ametamey, R. Schibli and W. Wadsak, *Org. Biomol. Chem.*, 2012, **10**, 3871–3874.
62 J.-H. Chun and V. W. Pike, *Chem. Commun.*, 2012, **48**, 9921–9923.
63 C. Philippe, J. Ungersboeck, E. Schirmer, M. Zdravkovic, L. Nics, M. Zeilinger, K. Shanab, R. Lanzenberger, G. Karanikas, H. Spreitzer, H. Viernstein, M. Mitterhauser and W. Wadsak, *Bioorg. Med. Chem.*, 2012, **20**, 5936–5940.
64 J. Ungersboeck, S. Richter, L. Collier, M. Mitterhauser, G. Karanikas, R. Lanzenberger, R. Dudczak and W. Wadsak, *Nucl. Med. Biol.*, 2012, **39**, 1087–1092.
65 S. Richter, V. Bouvet, M. Wuest, R. Bergmann, J. Steinbach, J. Pietzsch, I. Neundorf and F. Wuest, *Nucl. Med. Biol.*, 2012, **39**, 1202–1212.
66 G. K. Dewkar, G. Sundaresan, N. Lamichhane, J. Hirsch, C. Thadigiri, T. Collier, M. C. T. Hartman, G. Vaidyanthan and J. Zweit, *J. Labelled Compd. Radiopharm.*, 2013, **56**, 289–294.
67 S. H. Liang, T. L. Collier, B. H. Rotstein, R. Lewis, M. Steck and N. Vasdev, *Chem. Commun.*, 2013, **49**, 8755–8757.
68 L. Matesic, N. A. Wyatt, B. H. Fraser, M. P. Roberts, T. Q. Pham and I. Greguric, *J. Org. Chem.*, 2013, **78**, 11262–11270.
69 S. H. Liang, D. L. Yokell, R. N. Jackson, P. A. Rice, R. Callahan, K. A. Johnson, D. Alagille, G. Tamagnan, T. L. Collier and N. Vasdev, *MedChemComm*, 2014, **5**, 432–435.
70 G. Pascali, M. D. Simone, L. Matesic, I. Greguric and P. A. Salvadori, *J. Flow Chem.*, 2014, **4**, 86–91.
71 Y.-Y. Cheung, M. L. Nickels, D. Tang, J. R. Buck and H. C. Manning, *Bioorg. Med. Chem. Lett.*, 2014, **24**, 4466–4471.
72 S. H. Liang, D. L. Yokell, M. D. Normandin, P. A. Rice, R. N. Jackson, T. M. Shoup, T. J. Brady, G. E. Fakhri, T. L. Collier and N. Vasdev, *Mol. Imaging*, 2014, **13**, 7290.2014.00025.
73 R. C. Cumming, D. E. Olberg and J. L. Sutcliffe, *RSC Adv.*, 2014, **4**, 49529–49534.
74 M.-Q. Zheng, L. Collier, F. Bois, O. J. Kelada, K. Hammond, J. Ropchan, M. R. Akula, D. J. Carlson, G. W. Kabalka and Y. Huang, *Nucl. Med. Biol.*, 2015, **42**, 578–584.
75 S. Calderwood, T. L. Collier, V. Gouverneur, S. H. Liang and N. Vasdev, *J. Fluorine Chem.*, 2015, **178**, 249–253.
76 C. Philippe, D. Haeusler, T. Scherer, C. Fürnsinn, M. Zeilinger, W. Wadsak, K. Shanab, H. Spreitzer, M. Hacker and M. Mitterhauser, *EJNMMI Res.*, 2016, **6**, 31.
77 L. Matesic, A. Kallinen, I. Greguric and G. Pascali, *Nucl. Med. Biol.*, 2017, **52**, 24–31.
78 B. Zhang, G. Pascali, N. Wyatt, L. Matesic, M. A. Klenner, T. R. Sia, A. J. Guastella, M. Massi, A. J. Robinson and B. H. Fraser, *J. Labelled Compd. Radiopharm.*, 2018, **61**, 847–856.
79 S. Pfaff, C. Philippe, V. Pichler, M. Hacker, M. Mitterhauser and W. Wadsak, *Dalton Trans.*, 2018, **47**, 5997–6004.
80 L. Matesic, I. Greguric, G. Pascali, L. Matesic, I. Greguric and G. Pascali, *Aust. J. Chem.*, 2018, **71**, 811–817.
81 F. Menzel, J. Cotton, T. Klein, A. Maurer, T. Ziegler and J. M. Neumaier, *J. Flow Chem.*, 2023, **13**, 247–256.
82 J. M. Neumaier, A. Madani, T. Klein and T. Ziegler, *Beilstein J. Org. Chem.*, 2019, **15**, 558–566.
83 F. Menzel, T. Klein, T. Ziegler and J. M. Neumaier, *React. Chem. Eng.*, 2020, **5**, 1300–1310.
84 C.-C. Lee, G. Sui, A. Elizarov, C. J. Shu, Y.-S. Shin, A. N. Dooley, J. Huang, A. Daridon, P. Wyatt, D. Stout, H. C. Kolb, O. N. Witte, N. Satyamurthy, J. R. Heath, M. E. Phelps, S. R. Quake and H.-R. Tseng, *Science*, 2005, **310**, 1793–1797.
85 E. H. de Groot, N. Post, R. Boellaard, N. R. Wagenaar, A. T. Willemsen and J. A. van Dalen, *EJNMMI Res.*, 2013, **3**, 63.
86 A. M. Elizarov, R. M. van Dam, Y. S. Shin, H. C. Kolb, H. C. Padgett, D. Stout, J. Shu, J. Huang, A. Daridon and J. R. Health, *J. Nucl. Med.*, 2010, **51**, 282–287.
87 A. M. Elizarov, C. Meinhart, R. Miraghaie, R. M. van Dam, J. Huang, A. Daridon, J. R. Heath and H. C. Kolb, *Biomed. Microdevices*, 2011, **13**, 231–242.
88 A. Lebedev, R. Miraghaie, K. Kotta, C. E. Ball, J. Zhang, M. S. Buchsbaum, H. C. Kolb and A. Elizarov, *Lab Chip*, 2012, **13**, 136–145.
89 C. Rensch, S. Lindner, R. Salvamoser, S. Leidner, C. Böld, V. Samper, D. Taylor, M. Baller, S. Riese, P. Bartenstein, C. Wängler and B. Wängler, *Lab Chip*, 2014, **14**, 2556–2564.
90 X. Zhang, F. Liu, K.-A. Knapp, M. L. Nickels, H. C. Manning and L. M. Bellan, *Lab Chip*, 2018, **18**, 1369–1377.
91 X. Zhang, F. Liu, A. C. Payne, M. L. Nickels, L. M. Bellan and H. C. Manning, *Mol. Imaging Biol.*, 2020, **22**, 1370–1379.
92 R. Iwata, C. Pascali, K. Terasaki, Y. Ishikawa, S. Furumoto and K. Yanai, *J. Labelled Compd. Radiopharm.*, 2018, **61**, 540–549.
93 R. Iwata, C. Pascali, K. Terasaki, Y. Ishikawa, S. Furumoto and K. Yanai, *Appl. Radiat. Isot.*, 2017, **125**, 113–118.
94 S. Yu, *Biomed. Imaging Intervention J.*, 2006, **2**, e57.
95 M. R. Javed, S. Chen, J. Lei, J. Collins, M. Sergeev, H.-K. Kim, C.-J. Kim, R. M. van Dam and P. Y. Keng, *Chem. Commun.*, 2014, **50**, 1192–1194.
96 M. R. Javed, S. Chen, H.-K. Kim, L. Wei, J. Czernin, C.-J. "CJ" Kim, R. M. van Dam and P. Y. Keng, *J. Nucl. Med.*, 2014, **55**, 321–328.
97 R. Iwata, K. Terasaki, Y. Ishikawa, R. Harada, S. Furumoto, K. Yanai and C. Pascali, *Appl. Radiat. Isot.*, 2020, **166**, 109361.
98 Y. Lu, J. Wang, R. M. van Dam and A. Hsiao, *Chem. Eng. J.*, 2022, **435**, 134983.
99 C. Frank, G. Winter, F. Rensei, V. Samper, A. F. Brooks, B. G. Hockley, B. D. Henderson, C. Rensch and P. J. H. Scott, *EJNMMI Radiopharm. Chem.*, 2019, **4**, 24.

100 C. Frank, G. Winter, F. Rensei, V. Samper, P. Bartenstein, A. Brooks, B. Hockley, B. Henderson, S. Lindner, C. Rensch and P. Scott, *J. Nucl. Med.*, 2018, **59**, 671–671.
101 O. Ovdiichuk, Q. Béen, L. Tanguy and C. Collet, *React. Chem. Eng.*, 2023, **8**, 1476–1492.
102 O. Ovdiichuk, H. Mallapura, F. Pineda, V. Hourtané, B. Långström, C. Halldin, S. Nag, F. Maskali, G. Karcher and C. Collet, *Lab Chip*, 2021, **21**, 2272–2282.
103 H. Mallapura, L. Tanguy, B. Långström, L. L. Meunier, C. Halldin and S. Nag, *Molecules*, 2022, **27**, 8843.
104 O. Ovdiichuk, E. Roeder, S. Billotte, N. Veran and C. Collet, *Molecules*, 2022, **27**, 994.
105 P. Y. Keng, S. Chen, H. Ding, S. Sadeghi, G. J. Shah, A. Dooraghi, M. E. Phelps, N. Satyamurthy, A. F. Chatziioannou, C.-J. "CJ" Kim and R. M. van Dam, *Proc. Natl. Acad. Sci. U. S. A.*, 2012, **109**, 690–695.
106 S. Chen, M. R. Javed, H.-K. Kim, J. Lei, M. Lazari, G. J. Shah, R. M. van Dam, P.-Y. Keng and C.-J. "CJ" Kim, *Lab Chip*, 2014, **14**, 902–910.
107 S. A. Fiel, H. Yang, P. Schaffer, S. Weng, J. A. H. Inkster, M. C. K. Wong and P. C. H. Li, *ACS Appl. Mater. Interfaces*, 2015, **7**, 12923–12929.
108 K. Liu, E. J. Lepin, M.-W. Wang, F. Guo, W.-Y. Lin, Y.-C. Chen, S. J. Sirk, S. Olma, M. E. Phelps, X.-Z. Zhao, H.-R. Tseng, R. M. van Dam, A. M. Wu and C. K.-F. Shen, *Mol. Imaging*, 2011, **10**, 7290.2010.00043.
109 J. Wang and R. M. van Dam, *Mol. Imaging*, 2020, **19**, 1536012120973099.
110 A. A. Dooraghi, P. Y. Keng, S. Chen, M. R. Javed, C.-J. "CJ" Kim, A. F. Chatziioannou and R. M. van Dam, *Analyst*, 2013, **138**, 5654–5664.
111 M. C. Koag, H.-K. Kim and A. S. Kim, *J. Fluorine Chem.*, 2014, **166**, 104–109.
112 M. C. Koag, H.-K. Kim and A. S. Kim, *Chem. Eng. J.*, 2014, **258**, 62–68.
113 J. Wang, P. H. Chao, S. Hanet and R. M. van Dam, *Lab Chip*, 2017, **17**, 4342–4355.
114 J. Wang, P. H. Chao, R. Slavik and R. M. van Dam, *RSC Adv.*, 2020, **10**, 7828–7838.
115 A. Rios, J. Wang, P. H. Chao and R. M. van Dam, *RSC Adv.*, 2019, **9**, 20370–20374.
116 J. Wang, P. H. Chao and R. M. van Dam, *Lab Chip*, 2019, **19**, 2415–2424.
117 K. Lisova, J. Wang, T. J. Hajagos, Y. Lu, A. Hsiao, A. Elizarov and R. M. van Dam, *Sci. Rep.*, 2021, **11**, 20636.
118 K. Lisova, B. Y. Chen, J. Wang, K. M.-M. Fong, P. M. Clark and R. M. van Dam, *EJNMMI Radiopharm. Chem.*, 2019, **5**, 1.
119 J. Wang, T. Holloway, K. Lisova and R. M. van Dam, *React. Chem. Eng.*, 2020, **5**, 320–329.
120 K. Lisova, J. Wang, P. H. Chao and R. M. van Dam, *EJNMMI Radiopharm. Chem.*, 2020, **5**, 30.
121 A. Rios, T. S. Holloway, P. H. Chao, C. De Caro, C. C. Okoro and R. M. van Dam, *Sci. Rep.*, 2022, **12**, 10263.
122 J. Jones, V. Do, Y. Lu and R. M. van Dam, *Chem. Eng. J.*, 2023, **468**, 143524.
123 J. Wang, A. Rios, K. Lisova, R. Slavik, A. F. Chatziioannou and R. M. van Dam, *Nucl. Med. Biol.*, 2020, **82–83**, 41–48.
124 T. S. Laferriere-Holloway, A. Rios, G. Carlucci and R. M. van Dam, *Molecules*, 2022, **27**, 8178.
125 S. B. Campbell, Q. Wu, J. Yazbeck, C. Liu, S. Okhovatian and M. Radisic, *ACS Biomater. Sci. Eng.*, 2021, **7**, 2880–2899.
126 A. Zacheo, V. Arima, G. Pascali, P. A. Salvadori, A. Zizzari, E. Perrone, L. De Marco, G. Gigli and R. Rinaldi, *Microfluid. Nanofluid.*, 2011, **11**, 35–44.
127 A. M. Elizarov, *Lab Chip*, 2009, **9**, 1326–1333.
128 W.-Y. Tseng, J. S. Cho, X. Ma, A. Kunihiro, A. Chatziioannou and R. V. Dam, NSTI Nanotechnology Conference and Expo, *Toward Reliable Synthesis of Radiotracers for Positron Emission Tomography in PDMS Microfluidic Chips: Study and Optimization of the [18F]Fluoride Drying Process*, 2010, vol. 2, pp. 472–475.
129 L. Fernandez-Maza, B. Salvador, D. Orta, A. Corral and A. Luque, *Microfluid. Nanofluid.*, 2019, **23**, 109.
130 M. F. L'Annunziata, Ž. Grahek and N. Todorović, in *Handbook of Radioactivity Analysis*, ed. M. F. L'Annunziata, Academic Press, 4th edn, 2020, vol. 2, pp. 393–530.
131 R. Robertson, M. S. Germanos, C. Li, G. S. Mitchell, S. R. Cherry and M. D. Silva, *Phys. Med. Biol.*, 2009, **54**, N355.
132 J. S. Cho, R. Taschereau, S. Olma, K. Liu, Y.-C. Chen, C. K.-F. Shen, R. M. van Dam and A. F. Chatziioannou, *Phys. Med. Biol.*, 2009, **54**, 6757.
133 M. Lavén, S. Wallenborg, I. Velikyan, S. Bergström, M. Djodjic, J. Ljung, O. Berglund, N. Edenwall, K. E. Markides and B. Långström, *Anal. Chem.*, 2004, **76**, 7102–7108.
134 M. Lavén, I. Velikyan, M. Djodjic, J. Ljung, O. Berglund, K. Markides, B. Långström and S. Wallenborg, *Lab Chip*, 2005, **5**, 756–763.
135 S. Sadeghi, V. Liang, S. Cheung, S. Woo, C. Wu, J. Ly, Y. Deng, M. Eddings and R. M. van Dam, *Appl. Radiat. Isot.*, 2013, **75**, 85–94.
136 R. M. van Dam and A. F. Chatziioannou, *Front. Phys.*, 2021, 632056.
137 M. P. Taggart, M. D. Tarn, M. M. N. Esfahani, D. M. Schofield, N. J. Brown, S. J. Archibald, T. Deakin, N. Pamme and L. F. Thompson, *Lab Chip*, 2016, **16**, 1605–1616.
138 B. Salvador, D. A. E. Pineda, L. Fernandez-Maza, A. Corral, S. Camacho-Leon and A. Luque, *IEEE Sens. J.*, 2019, **19**, 7702–7707.
139 C. Fang, Y. Wang, N. T. Vu, W.-Y. Lin, Y.-T. Hsieh, L. Rubbi, M. E. Phelps, M. Müschen, Y.-M. Kim, A. F. Chatziioannou, H.-R. Tseng and T. G. Graeber, *Cancer Res.*, 2010, **70**, 8299–8308.
140 M. D. Tarn, D. Maneuski, R. Alexander, N. J. Brown, V. O'Shea, S. L. Pimlott, N. Pamme and S. J. Archibald, *Chem. Commun.*, 2016, **52**, 7221–7224.
141 M. D. Tarn, N. Y. Kızılyer, M. M. N. Esfahani, P. Joshi, N. J. Brown, N. Pamme, D. G. Jenkins and S. J. Archibald, *Chem. – Eur. J.*, 2018, **24**, 13749–13753.

142 G. Pratx, K. Chen, C. Sun, M. Axente, L. Sasportas, C. Carpenter and L. Xing, *J. Nucl. Med.*, 2013, **54**, 1841–1846.
143 G. Pratx, K. Chen, C. Sun, L. Martin, C. M. Carpenter, P. D. Olcott and L. Xing, *PLoS One*, 2012, **7**, e46285.
144 S. Türkcan, J. Nguyen, M. Vilalta, B. Shen, F. T. Chin, G. Pratx and P. Abbyad, *Anal. Chem.*, 2015, **87**, 6667–6673.
145 D. Maneuski, F. Giacomelli, C. Lemaire, S. Pimlott, A. Plenevaux, J. Owens, V. O'Shea and A. Luxen, *Appl. Radiat. Isot.*, 2017, **125**, 9–14.
146 A. M. Elizarov, in *Handbook of Radiopharmaceuticals*, John Wiley & Sons, Ltd, 2020, pp. 457–489.
147 QC1, **https://www.trasis.com/en/product/qc1/**, (accessed September 12, 2023).
148 J. Ly, N. S. Ha, S. Cheung and R. M. van Dam, *Anal. Bioanal. Chem.*, 2018, **410**, 2423–2436.
149 L. Patinglag, M. M. N. Esfahani, K. Ragunathan, P. He, N. J. Brown, S. J. Archibald, N. Pamme and M. D. Tarn, *Analyst*, 2020, **145**, 4920–4930.
150 L. L. Radford and S. E. Lapi, in *Radiopharmaceutical Chemistry*, ed. J. S. Lewis, A. D. Windhorst and B. M. Zeglis, Springer International Publishing, Cham, 2019, pp. 63–83.